J. Phys. Chem. A **2009,** *113,* 507–512

Electron Momentum Spectroscopy Study on Valence Electronic Structures of Ethylamine

Mi Yan, Xu Shan, Fang Wu, Xuexin Xia, Kedong Wang, Kezun Xu, and Xiangjun Chen*

Hefei National Laboratory for Physical Sciences at Microscale and Department of Modern Physics, University of Science and Technology of China, Hefei, 230026, China

Received: September 17, 2008; Revised Manuscript Received: November 12, 2008

The valence-shell binding energy spectra and electron momentum profiles of gaseous ethylamine are measured by (e, 2e) electron momentum spectroscopy. When taking into account the Boltzmann-weighted abundance of 39% for *trans* and 61% for two equivalent *gauche* conformers coexisted in ethylamine, the thermally averaged electron momentum profiles for all valence orbitals calculated using B3LYP method with 6-311++G** and aug-cc-pVTZ basis sets reproduce the experimental ones well, which supports that the *trans* conformer is more stable. In addition, the controversial ordering of 2a″ and 7a′ orbitals for the *trans* conformer is reassigned and an ionization band at about 13.7 eV, which was uncertain in previous literatures, is confirmed by comparing the experimental momentum profiles with the theoretical ones for the respective molecular orbitals. Furthermore, the ionization potentials and pole strengths for the inner valence orbitals are reported for the first time.

I. Introduction

Conformational phenomena are ubiquitous in multifarious molecules from simple molecules to complex biomolecules.[1−5] The conformational study, especially the determination of relative stability, has always been an attractive topic and also a challenging task in many cases.[6−14] Several techniques including infrared (IR) spectroscopy,[6−9] microwave (MW) spectroscopy,[10] Raman spectroscopy[11] and proton magnetic resonance (PMR) spectroscopy,[12] as well as electron diffraction (ED),[13] have yielded such information in previous literature. Recently, electron momentum spectroscopy[14] (EMS) also extends to this realm and opens new potential in exploring molecular conformations.[15−20] As a sequent work, we have carried out the EMS measurement on gaseous ethylamine.

Ethylamine (EA), one of the smallest molecules with distinct stable conformers, has one *trans* and two equivalent *gauche* rotamers due to the internal rotation of amino group about the C−N axis. The earlier conformational research of EA could trace to the far-infrared spectroscopy of Manocha et al.[8] and the *ab initio* calculation of Radom et al.[21] in which *gauche* conformer was predicted to be more stable than *trans* with the enthalpy differences of 104 cm^{-1} and 182 cm^{-1}, respectively, whereas at the same time, Tsuboi et al.[7] and Durig et al.,[11] who focused on IR and Raman spectroscopy studies, held the opposite view, i.e., *trans* conformer being more stable with the enthalpy differences of 230 cm^{-1} (2.75 kJ mol^{-1}) and 207 cm^{-1} (2.27 kJ mol^{-1}), respectively. Later on, the MW experiment of Fischer et al.,[10] the IR and ED experiments of Hamada et al.[6,13] and the MP2/6-311G** calculations of Zeroka et al.[22] all supported that the *trans* conformer is more stable, and presented quite consistent enthalpy differences with the values of 110 ± 50 cm^{-1} (1.32 ± 0.6 kJ mol^{-1}, MW), 100 ± 10 cm^{-1} (1.20 ± 0.12 kJ mol^{-1}, IR), 107 ± 70 cm^{-1} (1.28 ± 0.84 kJ mol^{-1}, ED) and 97 cm^{-1} (1.16 kJ mol^{-1}, calculation), respectively. Recently, more accurate enthalpy differences of 54 ± 4 cm^{-1} (0.65 ± 0.05 kJ mol^{-1}) were provided by the IR experiment of Durig et al.,[9] also upholding the *trans* being the more stable form.

Relative to the extensive research of molecular structures, on the other hand, detailed studies of electronic structures of EA are very scarce, and only reported by AL-Joboury et al.,[23] Katsumata et al.[24] and Maruyama et al.[25] using He I ultraviolet photoelectron spectroscopy (UPS) and Penning ionization electron spectroscopy (PIES). In these works, the ionization bands were assigned according to the symmetry of either *trans* or *gauche* conformer. A faint band (shoulder) at ∼13.7 eV in UPS was regarded to be somewhat uncertain by Katsumata et al.[24] and Maruyama et al.,[25] while it was ignored by AL-Joboury et al.[23] In addition, Katsumata et al.[24] assigned bands at 14.8 and 15.8 eV in UPS to the ionization from 7a′ and 2a″ orbitals with the ionization potential (IP) increasing, but the *ab initio* calculation of Kimura et al.[26] predicted the opposite ordering. It is noted that EMS has been proved to be an effective method of assigning unambiguously the orbital ordering due to its unique ability to obtain directly electron density distribution for individual molecular orbitals in momentum space.[27−30]

To our best knowledge, no EMS study of EA has been reported so far. In this article, we report the first EMS measurement on gaseous EA molecule. On the basis of the Boltzmann-weighted abundance of the conformers, the experimental electron momentum distributions are compared with the theoretical ones calculated by using density functional theory (DFT) with different-sized basis sets. The ordering of 2a″ and 7a′ orbitals for *trans*-conformer is reassigned, and the uncertain ionization band at about 13.7 eV in PES is confirmed. Moreover, the IPs and pole strengths for the main bands for the inner valence orbitals are obtained for the first time.

II. Experimental and Theoretical Background

Electron momentum spectroscopy[14] (EMS) is based on a kinematically complete (e, 2e) collision experiment in which an electron from target atoms or molecules is clearly knocked out by a high-energy incident electron and the residual ion acts as a spectator. According to conservations of energy and

---

* Corresponding author. Tel: 86-551-3601170. Fax: 86-551-3606266. E-mail: xjun@ustc.edu.cn.

10.1021/jp808281w CCC: $40.75

momentum in this process, the binding energy and the momentum of target electron can be expressed by

$$\varepsilon = E_0 - E_1 - E_2 \tag{1}$$

$$\boldsymbol{p} = \boldsymbol{p}_1 - \boldsymbol{p}_2 - \boldsymbol{p}_0 \tag{2}$$

where ε and $\boldsymbol{p}$ are the binding energy and the momentum of the target electron, and E_i and $\boldsymbol{p}_i$ (i = 0, 1, 2) are the energies and momenta of incident and two outgoing electrons, respectively.

The completely observable quantity in the EMS experiment is the triple differential cross section of the (e, 2e) reaction. Within the plane wave impulse approximation (PWIA), as well as the target Hartree–Fock (HF) or Kohn−Sham (KS) approximation, the cross section for the randomly oriented molecule can be described as[14,31]

$$\sigma \propto S_j^{(f)} \int \mathrm{d}\Omega_p |\psi_j(p)|^2 \tag{3}$$

where $\psi_j(p)$is the one-electron canonical HF or KS wave function in momentum space for the jth electron orbital from which the electron was knocked out. $S_j^{(f)}$, known as spectroscopic factor or pole strength, denotes the possibility of forming a one-hole configuration in the final state f. The integral in eq 3 is known as the spherically averaged electron density distributions in momentum space, i.e., electron momentum profiles.

The details of the present EMS spectrometer employing symmetric non-coplanar geometry have been described elsewhere.[32] Briefly, the gas phase target molecules are ionized by an impact with a high-energy electron beam generated by electron gun (E_0 = 1200 eV + binding energy). The scattered and ionized electrons having essentially equal energy (∼600 eV), and the same polar angles ($\theta_1 = \theta_2 = \theta = 45°$) are received by two hemispherical electron energy analyzers with a five-element cylindrical retarding lens, and are detected in coincidence by one-dimensional position sensitive detectors. The relative azimuthal angle ϕ between the two outgoing electrons is variable over a wide range (0° to ±30°) by rotating one energy analyzer around the direction of the incident electron beam and keeping the other analyzer fixed. In such arrangement, the quantity of target electron momentum is related to the relative azimuthal angle by[14]

$$p = \{(2p_1 \cos\theta - p_0)^2 + [2p_1 \sin\theta \sin(\phi/2)]^2\}^{1/2} \tag{4}$$

Before formal experiments, energy and momentum resolutions of the apparatus were determined to be ∼1.3 eV [full width at half-maximum (fwhm)] and ∼0.15 au by measuring Ar 3p ionization. The EA sample was purchased from the Sigma-Aldrich company with a stated purity greater than 99%. No impurities were observed in ionization spectra.

III. Computational Details

The potential energy curves for internal rotation of amino group about C−N bond, governing conformational interchange in EA, have been calculated early by Tsuboi et al.[7] and recently by Zeroka et al.[22] and Durig et al.[9] Three minima have been found. The one at the dihedral angle of 0° corresponds to the *trans* conformer while the other two at ±120 ° are two equivalent *gauche* conformers. Structural parameters and energy differences with thermodynamics corrections of *trans* and *gauche* conformers have been calculated systematically by Zeroka et al.[22] and Durig et al.[9] using different levels of theory and various sizes of basis sets. The results calculated by the second-order Møllet−Plesset perturbation (MP2) method with

TABLE 1: Experimental and Theoretical Ionization Energies for Valence Orbitals of Ethylamine[a]

	experimental				theoretical					
					OVGF/6-311++G**[b]		HF/6-311++G**[b]		SCF/4-31G[26]	
MO no.	HeI[24]	HeI[23]	HeI + PIES[25]	EMS[b]	*trans*	gauche	trans	gauche	trans	gauche
MO13	10a′ (9.50)	(9.19)	13a(10.0)	10a′/13a (9.5)[1.0]	10a′ (9.37)[0.92]	13a (9.45)[0.92]	10a′ (10.45)	13a (10.48)	10a′ (10.04)	13a (10.19)
MO12	3a″ (12.26)	(11.86)	12a(12.31)	3a″/12a (12.0)[1.0]	3a″ (12.49)[0.92]	12a (12.55)[0.92]	3a″ (13.20)	12a (13.34)	3a″(13.28)	12a (13.27)
MO11	9a′ (12.97)	(12.66)	11a(12.97)	9a′/11a (12.7)[1.0]	9a′ (12.99)[0.92]	11a (12.90)[0.92]	9a′ (13.86)	11a (13.90)	9a′ (13.85)	11a (13.67)
MO10	8a′ (13.80)[c]		10a(13.67)[c]	8a′/10a (13.6)[1.0]	8a′ (14.15)[0.91]	10a (13.25)[0.92]	8a′ (15.38)	10a (14.09)	8a′ (15.02)	10a (13.88)
MO9	7a′ (14.84)	(14.65)	9a(14.78)	7a′/ 9a (14.8)[1.0]	2a″ (14.71)[0.92]	9a (14.92)[0.92]	2a″ (15.62)	9a (15.93)	2a″(15.55)	9a (15.88)
MO8	2a″(15.80)	(15.55)	8a(15.88)	2a″/8a (15.8)[1.0]	7a′ (15.30)[0.91]	8a (16.02)[0.91]	7a′ (16.39)	8a (17.24)	7a′ (16.38)	8a (17.11)
MO7	1a″(16.77)	(16.81)	7a(16.86)	1a″/7a (16.9)[0.92]	1a″ (17.24)[0.91]	7a (16.95)[0.91]	1a″ (18.46)	7a (18.14)	1a″(18.41)	7a (17.95)
MO6		(19.71)		6a′/6a (20.2)[0.88]			6a′ (22.71)	6a (22.49)		
MO5				5a′/5a (23.4)[0.65]			5a′ (26.94)	5a (26.94)		
MO4				4a′/4a (27.5)[0.50]			4a′ (32.13)	4a (32.12)		

[a] Ionization energies (in eV) and pole strengths are listed in parentheses and square brackets. [b] This work. [c] This band was somewhat uncertain.

6-311G** or 6-311G(2df,2dp) basis sets are consistent with the experiments.[6,9]

The geometrical parameters of *trans* and *gauche* conformers are reoptimized in the present work by MP2 method with larger basis sets of aug-cc-pVTZ employing the GAUSSIAN 03 package of programs.[33] The optimized results are in good agreement with the previous values obtained by electron diffraction experiments of Hamada et al.[13] The theoretical electron momentum profiles (TMPs) for valence orbitals of *trans* and *gauche* conformers have been calculated within TKSA approximation according to eq 3. The corresponding position space KS wave functions are calculated by density functional theory employing B3LYP[34] hybrid functional combined with large basis sets of 6-311++G** and aug-cc-pVTZ. In order to compare with experimental results, the instrumental momentum resolution (i.e., angular resolution) has been folded into the TMPs utilizing the Gaussian-weighted planar grid method (GWPG).[35]

IV. Results and Discussion

Ethylamine ($CH_3CH_2NH_2$) contains 26 electrons occupying 13 molecular orbitals (MOs). On the basis of HF and B3LYP calculations, the ground electronic configurations of the *trans* conformer (C_s) and *gauche* conformer (C_1) can be written as

$$\underbrace{(1a')^2(2a')^2(3a')^2}_{\text{core shell}}\underbrace{(4a')^2(5a')^2(6a')^2}_{\text{inner valence}}\underbrace{(1a'')^2(7a')^2(2a'')^2(8a')^2(9a')^2(3a'')^2(10a')^2}_{\text{outer valence}}$$

and

$$\underbrace{(1a)^2(2a)^2(3a)^2}_{\text{core shell}}\underbrace{(4a)^2(5a)^2(6a)^2}_{\text{inner valence}}\underbrace{(7a)^2(8a)^2(9a)^2(10a)^2(11a)^2(12a)^2(13a)^2}_{\text{outer valence}}$$

The ionization potentials and pole strengths for outer valence orbitals of *trans* and *gauche* conformers have been calculated using the outer valence Green's function (OVGF)[36] method with the 6-311++G** basis set. The calculated results are listed in Table 1, together with the previous experimental values. It can be seen that OVGF calculations predict very close IPs for relevant MOs of *trans* and *gauche* conformers which give rise to the same ionization band in energy spectra. Compared with the experiment, OVGF calculations present more consistent IPs than HF.

A. Binding Energy Spectra. The binding energy spectra (BES) of EA over the energy range from 5 to 35 eV have been measured at 16 different relative azimuthal angles (ϕ): 0.5°, 1.5°, 2.5°, 3.5°, 4.5°, 5.5°, 6.5°, 7.5°, 8.5°, 9.5°, 11.5°, 13.5°, 15.5°, 17.5°, 19.5° and 23.5°, respectively. Figure 1 shows the individual BES for (a) $\phi = 0.5°$ and (b) $\phi = 8.5°$ and (c) summed for all 16 angles. It can be seen that six resolved structures have been observed obviously in BES. From a viewpoint of energies, the first three structures should be assigned to the transitions from seven outer valence orbitals while the last three correspond to three inner valence orbitals.

Although the bands for outer valence orbitals are not resolved entirely due to the low resolution of the EMS spectrometer, in order to check the controversial ordering of 2a″ and 7a′ orbitals and the uncertain ionization band at about 13.7 eV that appeared in previous literature,[24–26] seven Gaussian peaks (peaks 1–7 in Figure 1) have been employed to fit the first three structures in BES. The positions for each of the seven peaks are referred to the high-resolution UPS,[24,25] and the widths of individual peaks are the combinations of EMS instrumental energy resolution and Franck–Condon widths of ionization bands determined by UPS.[24,25] Slight adjustments have been used to compensate the asymmetry of the Franck–Condon profiles. For the last three structures in BES, three Gaussian peaks (peaks 8–10 in Figure 1) have been applied to fit the measured BES and therefore ionization energies for inner valence orbitals are determined to be 20.2, 23.4 and 27.5 eV for the first time.

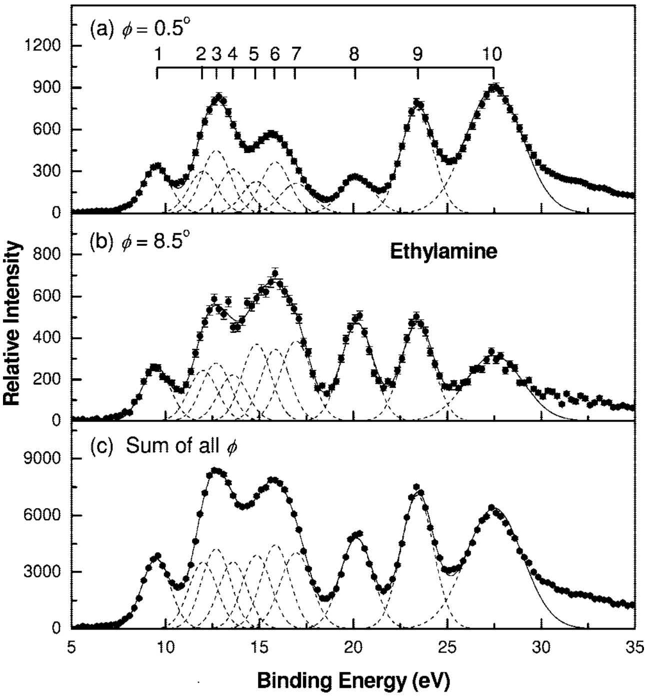

Figure 1. Binding energy spectra of ethylamine for (a) $\phi = 0.5°$, (b) $\phi = 8.5°$, and (c) the sum of all sixteen ϕ angles. The dashed lines represent Gaussian peaks fitting the BES. The solid line is the summed fit. The vertical bars indicate the positions of Gaussian peaks.

As mentioned above, *trans* and *gauche* conformers have very close orbital IPs for corresponding MOs, therefore the bands (peaks 1–10) in BES should be ascribed to the thermally averaged contributions from *trans* and *gauche* conformers. As shown in Figure 1, the first band (p1) at 9.5 eV corresponds to the ionization from the highest occupied molecular orbital (HOMO) of the EA molecule, which is the cooperative contribution of the 13a orbital of *gauche* and the 10a′ orbital of *trans* (denoted as MO13: 13a/10a′ for convenience of discussing). The bands (p2, p3) at 12.0 and 12.7 eV are assigned to MO12: 12a/3a″ and MO11: 11a/9a′, respectively. The assignment of the bands (p4, p5) at 13.6 and 14.8 eV, being inconsistent in previous studies,[24–26] will be discussed in next section. The bands (p6, p7) at 15.8 and 16.9 eV correspond to MO8: 8a/7a′ and MO7: 7a/1a″, respectively. The last three bands (p8, p9, p10) at 20.2 eV, 23.4 and 27.5 eV are owed to the ionization from MO6: 6a/6a′, MO5: 5a/5a′ and MO4: 4a/4a′, respectively. The determined ionization energies and band assignment are also presented in Table 1.

B. Electron Momentum Profiles. The experimental electron momentum profiles (XMPs) for each ionization peak (p1–10) are extracted by deconvoluting a series of angular correlated BES, and plotting area under the corresponding fitted peak as a function of momentum p (i.e., ϕ angle). The theoretical momentum profiles (TMPs) for valence orbitals of *trans* and *gauche* conformers have been obtained using the B3LYP method with 6-311++G** and aug-cc-pVTZ basis sets. When comparing the TMPs with the XMPs, the Boltzmann-weighted abundance of *trans* and *gauche* conformers should be taken into

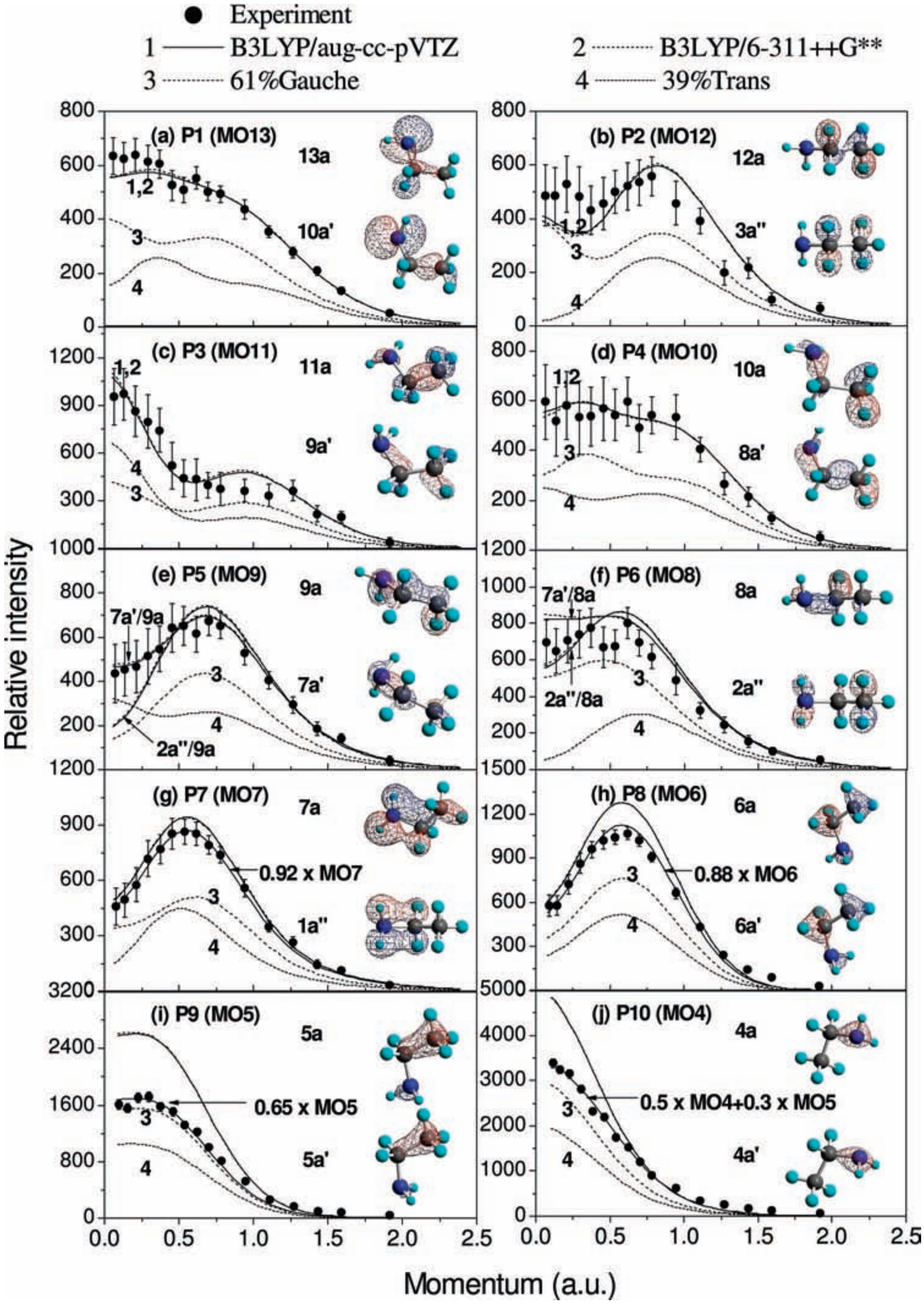

Figure 2. Experimental momentum profiles for valence bands (peaks 1−10) of ethylamine and the thermally averaged theoretical momentum profiles (TMPs) for *trans* (39%) and *gauche* (61%) conformers calculated using the B3LYP method with 6-311++G** and aug-cc-pVTZ basis sets, along with the individual TMPs and orbital maps for *trans* and *gauche* calculated by B3LYP/6-311++G**.

account. Furthermore, the XMPs and the thermally averaged TMPs are placed on a common intensity scale by normalizing the TMPs to the XMPs for HOMO (13a/10a′).

The relative abundance for *gauche* relative to *trans* conformer in EA was estimated to be 1.23 and 1.30 using enthalpy differences determined by the infrared experiment of Hamada et al.[6] and the MP2/6-311G** calculation of Zeroka et al.[22] Recently, more accurate relative abundance was deduced to be (61 ± 1)% for the two equivalent *gauche* conformers by the infrared spectra of Durig et al.[9] Therefore, relative abundances of 61% for *gauche* and 39% for *trans* have been employed in comparing TMPs with XMPs in the following discussions.

Figure 2 shows the XMPs for each ionization peak from valence orbitals of EA, together with the corresponding thermally averaged TMPs and individual TMPs for *trans* (39%) and *gauche* (61%) conformers calculated by the B3LYP method with 6-311++G** and aug-cc-pVTZ basis sets. The orbital maps for *trans* and *gauche* conformers calculated with B3LYP/6-311++G** are also plotted with a contour value of 0.05 in the right-hand side of each graph. It is noted that the error bars of experimental data given in Figure 2 represent the overall error of the statistical and deconvolution uncertainties.

As shown in Figure 2(a), the orbital map reveals that the HOMO (10a′ of *trans* and 13a of *gauche*) of EA is dominated by nitrogen lone pair with a little mixture of C−H or C−C bonds. The individual TMP for 13a orbital of *gauche* displays a mixed profile of "s-type" and "p-type" character (the so-called "sp-type"), and that of 10a′ orbital for *trans* is mainly "p-type" in nature. The thermally averaged TMPs (39% 10a′ and 61% 13a) calculated using aug-cc-pVTZ and 6-311++G** basis sets both show mainly "s-type" (slightly mixed with "p-type") character, well agreeing with the XMP except in the zero momentum region. Since the 13a orbital of *gauche* displays a π^*-like MO composed of N 2p lone-pair and two C−H bonds and such kind of MO was often observed higher intensity than the PIWA calculation in the low momentum region according to the previous EMS studies,[37−39] the discrepancy between the TMPs and XMPs at the origin of momentum should be possibly ascribed to distorted wave effects.

Figure 2(b) compares the XMP for peak 2 with the TMPs for MO12 (3a″/12a), along with the respective TMPs and orbital maps for *trans* and *gauche* conformers. It can be seen that the 3a″ orbital of *trans* exhibits a π^*-like MO composed of two pairs of asymmetric C−H bonds while the 12a orbital of *gauche* is the contribution of two pairs of C−H bonds with a little C−C bond. Consequently, the TMP for the 3a″ orbital of the *trans* conformer shows a pure "p-type" curve while that of the 12a orbital for *gauche* exposes an "sp-type" one. The thermally averaged TMPs of 10a′ (39%) and 13a (61%) are of "sp-type" character and consistent with the XMP in shape but underestimate the intensity in the low momentum region. Such a "turn up" phenomenon may also be ascribed to the distorted wave effect for 3a″ π^*-like MO according to the previous EMS studies.[37−39]

The XMP for peak 3 and the TMPs for MO11 (9a′/11a) are shown in Figure 2(c), together with the individual TMPs and orbital maps for *trans* and *gauche* conformers. It can be seen that the individual TMPs of 9a′ or 11a are both "sp-type" profiles and the thermally averaged TMPs for 9a′ and 11a are of "sp-type" character with two maxima at $p \sim 0$ au and $p \sim 1.0$ au and a saddle point at $p \sim 0.5$ au, which reproduce the XMP well except overestimating the intensity of the second maximum.

For the band at ∼13.6 eV, it was regarded to be somewhat uncertain in previous UPS stuides.[23−25] In order to check whether it occurs or not, the XMP for this band (p4) is also extracted individually although it is not resolved in BES. As shown in Figure 2(d), all the thermally averaged TMPs are in good agreement with the XMP, supporting that the band at ∼13.6 eV exists surely and is clearly assigned to the cooperative contribution of 8a′ of *trans* and 10a of *gauche*.

The XMP for the band (p5) at 14.8 eV is shown in Figure 2(e). Since the previous experimental and theoretical studies[24,26] presented controversial ordering of 2a″ and 7a′ for the *trans* conformer, the thermally averaged TMPs for 2a″/9a and 7a′/9a are both plotted in Figure 2(e). Compared with the XMP for p5, the TMPs of 7a′/9a is obviously more accordant with the XMP than that of 2a″/9a. This suggests the assignment of p5 to the ionization from 7a′/9a orbitals, supporting the UPS conclusion of Katsumata et al.[24] and different from the theoretical calculations. The XMP for the band (p6) at 15.8 eV together with the thermally averaged TMPs for 2a″/8a and 7a′/8a is presented in Figure 2(f). The thermally averaged TMPs for 2a″/8a reproduce the XMP of p6 better than that of 7a′/8a, which indicates that p6 is more likely assigned to the ionization from 2a″/8a and further supports the assignment of p5.

The band at 16.8 eV is assigned to 1a″/7a orbitals both contributed from the amino group. Due to the internal rotation of amino group, electron densities on amino group will *trans* or *gauche* to the C−H or C−C bonds and consequently bring different TMPs out. As shown in Figure 2(g), the thermally averaged TMPs well reproduce the shape of XMP for p7 but overestimate the experimental intensity. When the TMPs are multiplied by a factor of 0.92, they are in good accordance with the XMP. Such factor denotes the pole strength for the main transitions of ionization from 1a″/7a orbitals.

The last three bands (p8−10) at 20.2, 23.4 and 27.5 eV in BES are well resolved and assigned to the ionization from three inner valence orbitals, i.e., MO6: 6a/6a′, MO5: 5a/5a′ and MO4: 4a/4a′, respectively. The XMPs referring to these three peaks are shown in Figures 2(h)−(j), along with the TMPs and orbital maps for *trans* and *gauche* conformers. It can be seen that orbital maps for inner valence MO6, MO5 and MO4 display C−H bond, C−C bond and N 2s components, respectively. For MO6 and MO5, all the thermally averaged TMPs predict good shape of the XMPs but higher intensity. When the TMPs are scaled by a proper factor, good agreements between TMPs and XMPs can be achieved. Therefore, the pole strength for p8 and p9 is determined to be 0.88 and 0.65, respectively. But for the last one (p10), no matter how to change the factor, the TMP for MO4 disagrees with the XMP for p10, indicating that the satellite states from ionization of MO6 and MO5 may contribute to this band. It is common for inner valence orbitals due to the many-body interactions. We attempt to take the contribution from the nearby MO5 into account. The summed TMP ($0.5 \times \mathrm{MO4} + 0.3 \times \mathrm{MO5}$) can reproduce the XMP well. The stringent comparison needs the high level theoretical calculations such as the third-order algebraic diagrammatic construction [ADC(3)][40] or the symmetry adapted cluster-configuration interaction (SAC-CI).[41]

V. Summary

In this work, we report the first EMS measurement on valence-shell binding energy spectra and electron momentum profiles for gaseous ethylamine. When taking into account the relative abundance of 39% for *trans* and 61% for *gauche* conformers, the thermally averaged TMPs for complete valence orbitals calculated using B3LYP with 6-311++G** and aug-cc-pVTZ basis sets are generally consistent with the XMPs, indicating that such an abundance of 39% for *trans* in gaseous ethylamine is proper at room temprature and the *trans* is a more stable conformer. In addition, the controversial ordering of 2a″ and 7a′ orbitals for *trans*-conformer is assigned to be 7a′ and 2a″ with the order of increasing ionization energy. The uncertain band at ∼13.6 eV is confirmed to be surely in existence and is clearly assigned to the cooperative contribution of 8a′ of *trans* and 10a of *gauche*. Furthermore, the ionization potentials and pole strengths for the inner valence orbitals have been obtained for the first time.

Acknowledgment. This work was supported by National Natural Science Foundation of China (Grant Nos. 10734040 and 10474090). The authors also gratefully acknowledge Professor C. E. Brion from the University of British Columbia (UBC) in Canada for supplying the HEMS and RESFOLD programs.

References and Notes

(1) Tarnovsky, A. N.; Sundstrom, V.; Akesson, E.; Pascher, T. *J. Phys. Chem. A* **2004**, *108*, 237.

(2) Ha, T. K.; Gunthard, H. H. *J. Am. Chem. Soc.* **1993**, *115*, 11939.

(3) Akasaka, T.; Wakahara, T.; Nagase, S.; et al. *J. Phys. Chem. B* **2001**, *105*, 2971.

(4) Satink, R. G.; Meijer, G.; von Helden, G. *J. Am. Chem. Soc.* **2003**, *125*, 15714.

(5) Dugourd, Ph.; Hudgins, R. R.; Tenenbaum, J. M. *Phys. Rev. Lett.* **1998**, *80*, 4197.

(6) Hamada, Y.; Hashiguchi, K. *J. Mol. Spectrosc.* **1983**, *102*, 123.

(7) Tsuboi, M.; Tamagake, K. *J. Chem. Phys.* **1975**, *63*, 5177.

(8) Manocha, A. S.; Tuazon, E. C. *J. Phys. Chem.* **1974**, *78*, 803.

(9) Durig, J. R.; Zhang, C.; K.Gounev, T. *J. Phys. Chem. A* **2006**, *110*, 5674.

(10) (a) Fischer, E.; Botaskor, I. *J. Mol. Spectrosc.* **1982**, *91*, 116. (b) Fischer, E.; Botaskor, I. *J. Mol. Spectrosc.* **1984**, *104*, 226.

(11) Durig, J. R.; Li, Y. S. *J. Chem. Phys.* **1975**, *63*, 4110.

(12) Bothner-By, A. A.; Naar-Colin, C. *J. Am. Chem. Soc.* **1961**, *83*, 231.

(13) Hamada, Y.; Tsuboi, M. *J. Mol. Struct.* **1986**, *146*, 253.

(14) (a) McCarthy, I. E.; Weigold, E. *Rep. Prog. Phys.* **1991**, *54*, 789. (b) Brion, C. E. *Int. J. Quantum Chem.* **1986**, *29*, 1397. (c) Coplan, M. A.; Moore, J. H.; Doering, J. P. *Rev. Mod. Phys.* **1994**, *66*, 985.

(15) Mathers, C. P.; Gover, B. N.; Ying, J. F.; Zhu, H.; Leung, K. T. *J. Am. Chem. Soc.* **1994**, *116*, 7250.

(16) (a) Zheng, Y.; Neville, J. J.; Brion, C. E. *Science* **1995**, *270*, 786. (b) Neville, J. J.; Zheng, Y.; Brion, C. E. *J. Am. Chem. Soc.* **1996**, *118*, 10533.

(17) (a) Deleuze, M. S.; Pang, W. N.; Salam, A.; Shang, R. C. *J. Am. Chem. Soc.* **2001**, *123*, 4049. (b) Deleuze, M. S.; Knippenberg, S. *J. Chem. Phys.* **2006**, *124*, 104309.

(18) (a) Wang, F.; Downton, M. *J. Phys. B: At. Mol. Opt. Phys.* **2004**, *37*, 557. (b) Wang, F. *J. Phys. Chem. A* **2003**, *107*, 10199.

(19) Yang, T. C.; Su, G. L.; Ning, C. G.; Deng, J. K.; Wang, F.; Zhang, S. F.; Ren, X. G.; Huang, Y. R. *J. Phys.Chem. A* **2007**, *111*, 4927.

(20) Wu, F.; Chen, X. J.; Shan, X.; Tian, S. X.; Li, Z. J.; Xu, K. Z. *J. Phys. Chem. A* **2008**, *112*, 4360.

(21) Radom, L.; Hehre, W. J.; Pople, J. *J. Am, Chem. Soc.* **1972**, *94*, 2371.

(22) (a) Zeroka, D.; Jensen, J. O.; Samuels, A. C. *J. Phys. Chem. A* **1998**, *102*, 6571. (b) Zeroka, D.; Jensen, J. O. *J. Mol. Struct. (THEOCHEM)* **1999**, *465*, 119.

(23) AL-Joboury, M. I.; Turner, D. W. *J. Chem. Soc.* **1964**, 4434.

(24) Katsumata, S.; Iwai, T.; Kimura, K. *Bull. Chem. Soc. Jpn.* **1973**, *46*, 3391.

(25) Maruyama, R.; Ohno, K. *J. Phys. Chem.* **2004**, *108*, 4211.

(26) Kimura, K.; Katsumata, S.; Achiba, Y.; Yamazaki, T.; Iwata, S. *Handbook of HeI photoelectron spectra of fundamental organic molecules*; Japan Scientific Societies Press: Tokyo, 1981; p 11.

(27) Chen, X. J.; Zhou, L. X.; Zhang, X. H.; Yin, X. F.; Xu, C. K.; Shan, X.; Wei, Z.; Xu, K. Z. *J. Chem. Phys.* **2004**, *120*, 7933.

(28) Takahashi, M.; Ogino, R.; Udagawa, Y. *Chem. Phys. Lett.* **2004**, *120*, 7933.

(29) Ning, C. G.; Ren, X. G.; Deng, J. K.; Su, G. L.; Zhang, S. F.; Huang, F.; Li, G. Q. *Chin. Phys.* **2005**, *14*, 2467.

(30) Shan, X.; Chen, X. J.; Zhou, L. X.; Li, Z. J.; Liu, T.; Xue, X. X.; Xu, K. Z. *J. Chem. Phys.* **2006**, *125*, 154307.

(31) Duffy, P.; Chong, D. P.; Casida, M. E.; Salahub, D. R. *Phys. Rev. A* **1994**, *50*, 4707.

(32) Yang, B. X.; Chen, X. J.; Pang, W. N.; Chen, M. H.; Zhang, F.; Tian, B. L.; Xu, K. Z. *Acta Phys. Sin.* **1997**, *5*, 862.

(33) Frisch, M. J.; Trucks, G. W.; Schlegel, H. B.; *GAUSSIAN 03, Revision B.04*; Gaussian, Inc.: Pittsburgh, PA, 2003.

(34) (a) Becke, A. D. *J. Chem. Phys.* **1993**, *98*, 5648. (b) Lee, C.; Yang, W.; Parr, R. G. *Phys. Rev. B* **1988**, *37*, 785.

(35) Duffy, P.; Casida, M. E.; Brion, C. E.; Chong, D. P. *Chem. Phys.* **1992**, *159*, 347.

(36) (a) Cederbaum, L. S. *J. Phys. B* **1975**, *8*, 290. (b) von Niessen, W.; Schirmer, J.; Cederbaum, L. S. *Comput. Phys. Rep.* **1984**, *1*, 57. (c) Zakrzewski, V. G.; Ortiz, J. V.; Nichols, J. A.; Heryadi, D.; Yeager, D. L.; Golab, J. T. *Int. J. Quantum Chem.* **1996**, *60*, 29.

(37) Brion, C. E.; Zheng, Y.; Rolke, J.; Neville, J. J.; McCarthy, I. E.; Wang, J. *J. Phys. B* **1998**, *31*, L223.

(38) Litvinyuk, I. V.; Zheng, Y.; Brion, C. E. *Chem. Phys.* **2000**, *253*, 41.

(39) Ren, X. G.; N ing, C. G.; Deng, J. K.; Zhang, S. F.; Su, G. L.; Huang, F.; Li, G. Q. *Phys. Rev. Lett.* **2005**, *94*, 163201.

(40) (a) Schirmer, J.; Cederbaum, L. S.; Walter, O. *Phys. Rev. A* **1983**, *28*, 1237. (b) von Niessen, W.; Schirmer, J.; Cederbaum, L. S. *Comput. Phys. Rep.* **1984**, *1*, 57. (c) Schirmer, J.; Angonoa, G. *J. Chem. Phys.* **1989**, *91*, 1754. (d) Weikert, H.-G.; Meyer, H.-D.; Cederbaum, L. S.; Tarantelli, F. *J. Chem. Phys.* **1996**, *104*, 7122. (e) Deleuze, M. S.; Giuffreda, M. G.; Francois, J.-P.; Cederbaum, L. S. *J. Chem. Phys.* **1999**, *111*, 5851. (f) Deleuze, M. S. *Int. J. Quantum Chem.* **2003**, *93*, 191.

(41) (a) Nakatsuji, H.; Hirao, K. *J. Chem. Phys.* **1978**, *68*, 2053. (b) Nakatsuji, H. *J. Chem. Phys.* **1985**, *83*, 713. (c) Nakatsuji, H. *J. Chem. Phys.* **1985**, *83*, 5743. (d) Nakatsuji, H. *J. Chem. Phys.* **1991**, *94*, 6716. (e) Nakatsuji, H. *Computational Chemistry—Review of Current Trends*; World Scientific: Singapore, 1997; Vol. 2, pp 62−124.

JP808281W